Topology Optimization of Actuators Using Structural Flexibility

Shinji Nishiwaki, Emílio Carlos Nelli Silva, Kazuhiro Saitou, and Noboru Kikuchi
The University of Michigan

1. Abstract

A mechanical structure obtains additional functions such as the kinematic function if we can specify the deformed shape at the specified portion of the mechanical structure. This flexible structure is used as a new type of mechanisms which are called compliant mechanisms. A mechanical resonator can be designed by extending the concept of compliant mechanisms to the dyanmic case. We can also design an actuator or a mechanical sensor by combining the flexible structure with energy converting devices such as piezoceramic. In this study, we shall discuss the topology optimization method which provides a mechanical structure with the kinematic function for the design of the flextensional actuators and resonators in MEMS. First, we formulate the kinematic function and its sensitivity with respect to a design variable. Next, we formulate the multi-objective optimization problem in order to obtain an optimal solution incorporating this function and stiffness. Based on these formulations and the homogenization method, the optimization procedure is constructed. Finally, some design examples are presented to confirm that the design method proposed here satisfy the problem.

2. Keywords

Topology optimization, The homogenization method, Flextensional actuators, MEMS (Micro-Electro-Mechanical-Systems)

3. Formulation of Kinematic Function

The kinematic function is formulated using a mutual energy concept. This concept is based on the so-called reciprocal theorem (or Betti's theorem). This formulation is extended to the dynamic case for the design of resonators in MEMS.

Kinematic Function for the Design of Flextensional Actuators

Consider a linear elastic domain, Ω, which has the piezoelectric effect as shown in Figure 1 (a). Suppose that the domain is fixed at boundary Γ_d, and the electric potential is set to zero at boundary Γ_ϕ. Let us consider the two cases, Case (a) and Case (b). In Case (a), the domain is subjected to surface charge q^1 at boundary Γ_{q^1}, and in Case (b), it is subjected to boundary traction $\boldsymbol{t}^2$ at boundary Γ_{t^2}. Body forces applied to the elastic domain are ignored for simplicity in the formulation. The displacement field is $\boldsymbol{u}^1$, and the electric potential is ϕ^1 in Case (a), and $\boldsymbol{u}^2$ and ϕ^2, respectively, in Case (b). We assume that traction $\boldsymbol{t}^2$ is a unit dummy load. Then, the following linear form defined as the mean transduction can be interpreted as the measure of the kinematic function:

$$l\left\langle \boldsymbol{t}^2, \boldsymbol{u}^1 \right\rangle = \int_{\Gamma_{t^2}} \boldsymbol{t}^2 \bullet \boldsymbol{u}^1 d\Gamma \tag{1}$$

If $l\left\langle \boldsymbol{t}^2, \boldsymbol{u}^1 \right\rangle$ is sufficiently large, then sufficient flexibility in the direction of $\boldsymbol{t}^2$ due to electric charge is obtained. Furthermore, the sensitivity of $l\left\langle \boldsymbol{t}^2, \boldsymbol{u}^1 \right\rangle$ with respect a design variable A is obtained as follows:

$$\frac{\partial L\left\langle \boldsymbol{t}^2, \boldsymbol{u}^1 \right\rangle}{\partial A} = -\int_\Omega \varepsilon\left(\boldsymbol{u}^1\right)^T \frac{\partial \boldsymbol{E}}{\partial A} \varepsilon\left(\boldsymbol{u}^2\right) d\Omega - \int_\Omega \varepsilon\left(\boldsymbol{u}^1\right)^T \frac{\partial \boldsymbol{e}^P}{\partial A} \nabla \phi^2 d\Omega - \int_\Omega \varepsilon\left(\boldsymbol{u}^2\right)^T \frac{\partial \boldsymbol{e}^P}{\partial A} \nabla \phi^1 d\Omega + \int_\Omega \nabla \phi^{1\,T} \frac{\partial \varepsilon^s}{\partial A} \nabla \phi^2 d\Omega \tag{2}$$

where $\varepsilon(\boldsymbol{u})$ is the infinitesimal strain with respect to displacement field $\boldsymbol{u}$, $\boldsymbol{E}$ is the elasticity tensor, $\boldsymbol{e}^p$ is the piezoelectric strain tensor, and $\boldsymbol{e}^S$ is the free-body electric tensor.

Kinematic Function for the Design of Resonators in MEMS

Consider a linear elastic domain, Ω, as shown in Figure 1 (b). Now, consider the two cases, Case (a) and Case (b). In Case (a), the elastic domain is subjected to boundary traction $\boldsymbol{t}^1$ at boundary Γ_{t^1}, and in Case (b), it is subjected to boundary traction $\boldsymbol{t}^2$ at boundary Γ_{t^2}. Body forces applied to the elastic domain are ignored for simplicity in the formulation. The displacement field are $\boldsymbol{u}^1$ in Case (a), and $\boldsymbol{u}^2$ in Case (b). We suppose that tractions $\boldsymbol{t}^1$ and $\boldsymbol{t}^2$ are harmonic excitations to the elastic domain, and displacement fields $\boldsymbol{u}^1$ and $\boldsymbol{u}^2$ are also harmonic in the steady state. That is, tractions, $\boldsymbol{t}^1$ and $\boldsymbol{t}^2$, and displacement fields, $\boldsymbol{u}^1$ and $\boldsymbol{u}^2$, are assumed to be described as $\boldsymbol{t}^1 = \boldsymbol{T}^1 e^{j\omega t}$, $\boldsymbol{t}^2 = \boldsymbol{T}^2 e^{j\omega t}$, $\boldsymbol{u}^1 = \boldsymbol{U}^1 e^{j\omega t}$, and $\boldsymbol{u}^2 = \boldsymbol{U}^2 e^{j\omega t}$, where ω stands for an excitation frequency, t stands for time, and $\boldsymbol{T}^1$, $\boldsymbol{T}^2$, $\boldsymbol{U}^1$, and $\boldsymbol{U}^2$ stand for amplitudes of $\boldsymbol{t}^1$, $\boldsymbol{t}^2$, $\boldsymbol{u}^1$, and $\boldsymbol{u}^2$, respectively. Here, the linear form implying the mutual mean compliance in the dynamic case defined by

$$l\left\langle \boldsymbol{T}^2, \boldsymbol{U}^1 \right\rangle = \int_{\Gamma_{t^2}} \boldsymbol{T}^2 \bullet \boldsymbol{U}^1 d\Gamma \tag{3}$$

can be interpreted as the measure of the kinematic function in the dynamic case. If the absolute value of $l\left\langle \boldsymbol{T}^2, \boldsymbol{U}^1 \right\rangle$ is sufficiently large, then sufficient flexibility in the direction of $\boldsymbol{t}^2$ due to traction $\boldsymbol{t}^1$ is obtained. Furthermore, the sensitivity of $l\left\langle \boldsymbol{T}^2, \boldsymbol{U}^1 \right\rangle$ with respect a design variable A is obtained as follows:

$$\frac{\partial l\langle \boldsymbol{T}^2, \boldsymbol{U}^1\rangle}{\partial A} = -\int_\Omega \varepsilon(\boldsymbol{U}^1)^T \frac{\partial \boldsymbol{E}}{\partial A}\varepsilon(\boldsymbol{U}^2) d\Omega + \omega^2 \int_\Omega \frac{\partial \rho}{\partial A}\boldsymbol{U}^2 \bullet \boldsymbol{U}^1 d\Omega \tag{4}$$

where ρ is the mass density.

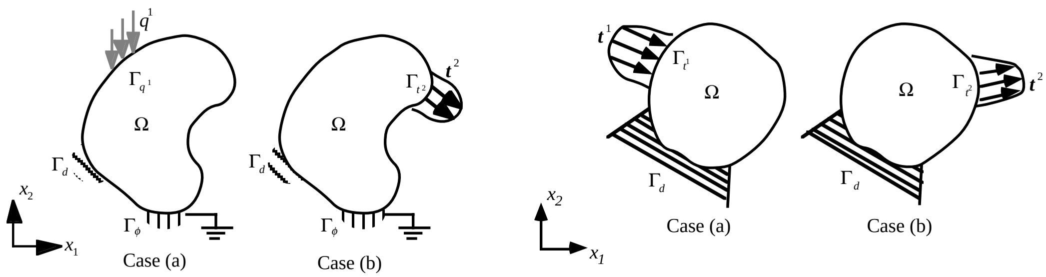

(a) A domain subjected to electric charge and traction   (a) A domain subjected to two periodic tractions

Figure 1. Definition of kinematic function

4. Homogenization Design Method

The homogenization design method is a topology optimization method which uses a concept of an extended design domain D shown in Figure 2 (a) and the following characteristic function:

$$\chi_\Omega(\boldsymbol{x}) = \begin{cases} 1 & \text{if } \boldsymbol{x} \in \Omega_d \\ 0 & \text{if } \boldsymbol{x} \in D \setminus \Omega_d \end{cases} \tag{5}$$

where $\boldsymbol{x}$ is a specified position in the design domain, and Ω_d is an original design domain. Using this function, the original structural design problem is replaced with the material distribution problem. The homogenization method is utilized for the relaxation of the extended design domain. Figure 2 (b) shows a microstructure which is formed inside an empty rectangle in a unit cell, where α, β, and θ are regarded as the design variables**.**

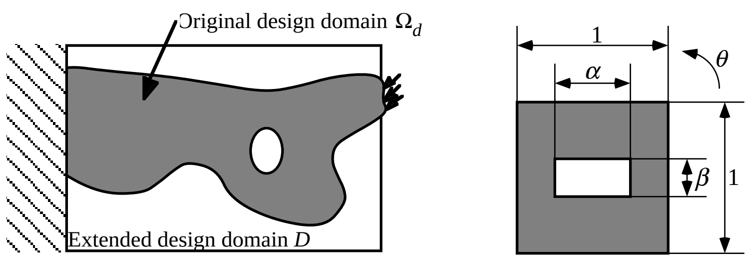

(a) Fixed and extended design domain   (b) Microstructure

Figure 2. Extended design domain and microstructure

5. Formulation of Multi-objective Optimization Problem

<u>Design of Flextensional Actuator</u>

Suppose that the original design domain Ω_d is fixed at boundary Γ_d, and the electric potential is set to zero at boundary Γ_ϕ in the piezoceramic device. The piezoceramic device is subjected to surface charge q^1 at boundary Γ_{q^1}, as shown in Figure 3 (a). We design a flextensional actuator which deforms in the specified direction $\boldsymbol{t}^2$ at boundary Γ_{t^2} due to surface charge q^1 at boundary Γ_{q^1}, and has sufficient stiffness at boundary Γ_{t^2} in order to a reaction force caused by a workpiece. The kinematic function is obtained by maximizing the mean transduction, posed by traction $\boldsymbol{t}^2$ and the displacement field $\boldsymbol{u}^1$ due to surface charge q^1 (Case(a)). Sufficient stiffness is obtained by minimizing the mean compliance at boundary Γ_{t^2} posed by traction $-\boldsymbol{t}^2$, while the electric potential is set to zero at boundary Γ_{q^1} (Case (b)). Therefore, the optimization problem is formulated as follows:

$$\underset{\alpha,\beta,\text{ and }\theta}{\text{maximize}}\ l\langle \boldsymbol{t}^2, \boldsymbol{u}^1\rangle = \int_{\Gamma t^2} \boldsymbol{t}^2 \bullet \boldsymbol{u}^1 d\Gamma \text{ and } \underset{\alpha,\beta,\text{ and }\theta}{\text{minimize}}\ l\langle \boldsymbol{t}^3, \boldsymbol{u}^3\rangle = \int_{\Gamma t^2} \boldsymbol{t}^3 \bullet \boldsymbol{u}^3 d\Gamma \tag{6}$$

subject to

$$\boldsymbol{t}^3 = -\boldsymbol{t}^2 \tag{7}$$

$$\text{equilibrium equations} \tag{8}$$

$$0 \le \alpha \le 1 \tag{9}$$

$$0 \le \beta \le 1 \tag{10}$$

$$g(\rho_v) = \int_{\Omega_d} \rho_v d\Omega - \Omega_s = \int_{\Omega_d} (1-\alpha\beta) d\Omega - \Omega_s \le 0 \tag{11}$$

where ρ_v is the volumetric density, and Ω_S is the total volume constraint of the solid material forming the porous structure. In order to obtain an appropriate optimal configuration incorporating the two functions defined by Equation (6), the following multi-objective function is proposed:

$$\underset{\alpha,\beta,\text{ and }\theta}{\text{maximize}} \ f_1 = \frac{l\langle \boldsymbol{t}^2, \boldsymbol{u}^1 \rangle}{l\langle \boldsymbol{t}^3, \boldsymbol{u}^3 \rangle} \tag{12}$$

more generally,

$$\underset{\alpha,\beta,\text{ and }\theta}{\text{maximize}} \ f_2 = W \log\left(l\langle \boldsymbol{t}^2, \boldsymbol{u}^1 \rangle \right) - (1-W)\log\left(l\langle \boldsymbol{t}^3, \boldsymbol{u}^3 \rangle \right) \tag{13}$$

where W is a weighting coefficient such that $0 \le W \le 1$.

<u>Design of Resonator</u>

Suppose that the original design domain of a flexible structure Ω_d is fixed at boundary Γ_d and is subjected to the periodically oscillating boundary traction $\boldsymbol{t}^1 = \boldsymbol{T}^1 e^{j\omega t}$, where ω is an excitation frequency and t is time, as shown in.Figure 3 (b).We design a resonator which deforms along a direction specified by unit dummy vector $\boldsymbol{T}^2$, where $\boldsymbol{t}^2 = \boldsymbol{T}^2 e^{j\omega t}$, and has sufficient stiffness at boundaries Γ_{t^1} and Γ_{t^2} in order to resist an applied force and a reaction force, respectively. The kinematic function is obtained by maximizing the absolute value of mutual mean compliance, posed by traction $\boldsymbol{t}^2$ and the displacement field $\boldsymbol{u}^1$ due to boundary traction $\boldsymbol{t}^1$(Case(a)). Sufficient stiffness at boundary Γ_{t^1} is obtained by minimizing the absolute value of mean compliance posed by traction $\boldsymbol{t}^1$, while boundary Γ_{t^2} is fixed (Case (b)). Moreover, sufficient stiffness at boundary Γ_{t^2} is obtained by minimizing the absolute value of the mean compliance posed by traction -$\boldsymbol{t}^2$, while boundary Γ_{t^1} is fixed (Case (c)). Therefore, the optimization problem is formulated as follows:

$$\begin{gathered}\underset{\alpha,\ \beta,\text{ and }\theta}{\text{maximize}} \left| l\langle \boldsymbol{T}^2, \boldsymbol{U}^1 \rangle \right| = \left| \int_{\Gamma t^2} \boldsymbol{T}^2 \bullet \boldsymbol{U}^1 d\Gamma \right|, \quad \underset{\alpha,\beta,\text{ and }\theta}{\text{minimize}} \left| l\langle \boldsymbol{T}^3, \boldsymbol{U}^3 \rangle \right| = \left| \int_{\Gamma t^1} \boldsymbol{T}^3 \bullet \boldsymbol{U}^3 d\Gamma \right|, \\ \text{and } \underset{\alpha,\beta,\text{ and }\theta}{\text{minimize}} \left| l\langle \boldsymbol{T}^4, \boldsymbol{U}^4 \rangle \right| = \left| \int_{\Gamma t^2} \boldsymbol{T}^4 \bullet \boldsymbol{U}^4 d\Gamma \right| \end{gathered} \tag{14}$$

subject to

$$\boldsymbol{T}^3 = \boldsymbol{T}^1 \tag{15}$$

$$\boldsymbol{T}^4 = -\boldsymbol{T}^2 \tag{16}$$

$$\text{equilibrium equations} \tag{17}$$

$$0 \le \alpha \le 1 \tag{18}$$

$$0 \le \beta \le 1 \tag{19}$$

$$g(\rho_v) = \int_{\Omega_d} \rho_v d\Omega - \Omega_s = \int_{\Omega_d} (1-\alpha\beta) d\Omega - \Omega_s \le 0 \tag{20}$$

In order to obtain an appropriate optimal configuration incorporating the three functions defined by Equation (14), the following multi-objective function is proposed:

$$\underset{\alpha,\beta,\text{ and }\theta}{\text{maximize}} \ f_3 = W \log\left| l\langle \boldsymbol{T}^2, \boldsymbol{U}^1 \rangle \right| - \frac{1}{2}(1-W)\log\left(w_s l\langle \boldsymbol{T}^3, \boldsymbol{U}^3 \rangle^2 + (1-w_s) l\langle \boldsymbol{T}^4, \boldsymbol{U}^4 \rangle^2 \right) \tag{21}$$

where w_S is a weighting coefficient such that $0 \le w_s \le 1$.

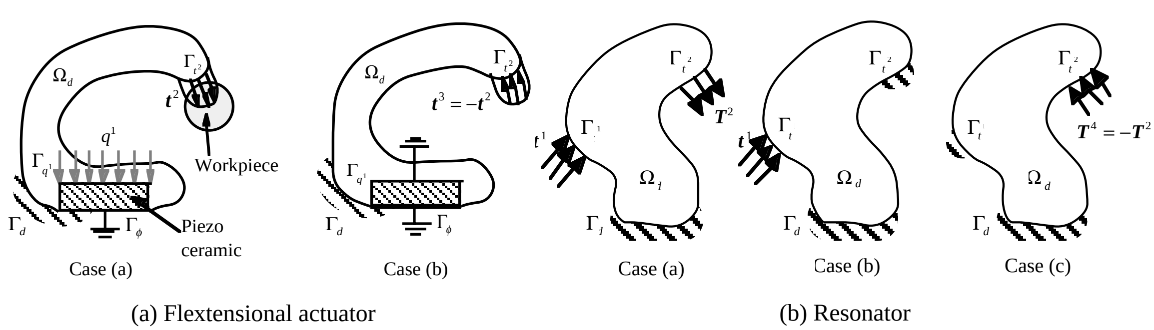

Figure 3. Design Specifications

6. Optimization Procedure

Figure 4 shows a flowchart of the optimization procedure. First, the homogenized coefficients for elasticity tensor $\boldsymbol{E}^H$ are calculated using the homogenization method. Next, the extended design domain D is discretized using the finite elements. In this discretization scheme, we approximate that the configuration of the microstructure is the same inside the element. Therefore, we have three design variables, α_i, β_i, and θ_i, for i=1,...,n where n is the number of the elements. The objective functions, constraints, and their sensitivities with respect α_i and β_i, are computed using FEM. The sequential linear programming (SLP) is utilized to solve the optimization problem. This is because SLP can handle numerous design variables (more than 10,000), and it requires only the sensitivities of the objective functions and constraints, although the fast convergence cannot be expected. Finally, the angle θ_i is practically updated to the principal direction of the stress to minimize the mean compliance, $l\left\langle \boldsymbol{t}^3, \boldsymbol{u}^3 \right\rangle$, in the case of the flextensional design, and is practically updated to the principal direction of the stress to minimize the larger mean compliance between $l\left\langle \boldsymbol{T}^3, \boldsymbol{U}^3 \right\rangle$ and $l\left\langle \boldsymbol{T}^4, \boldsymbol{U}^4 \right\rangle$ using the multi-loading criterion which was proposed by Suzuki and Kikuchi in the case of the resonator design

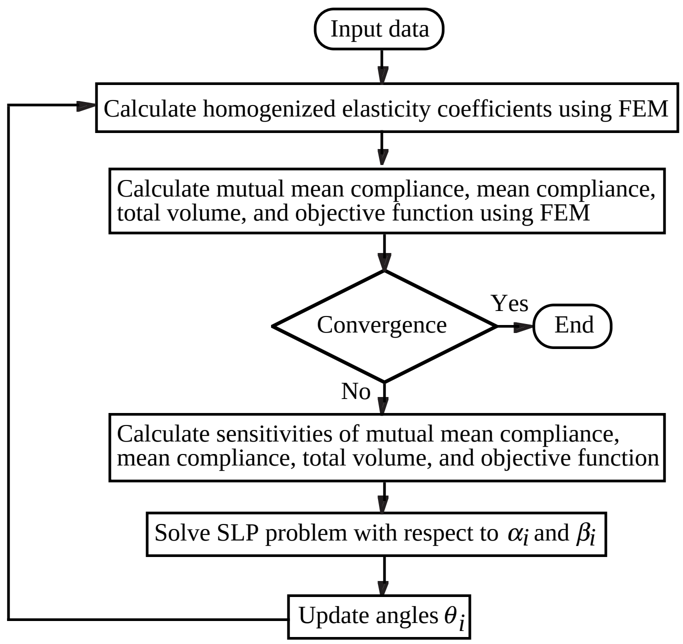

Figure 4. Flowchart of optimization procedure

7. Numerical Examples

<u>Design of Flextensional Actuator</u>

Figure 5 (a) shows a design domain of a actuator. The deformations at points P_2 in the directions of dummy loads $\boldsymbol{F}^2$ is maximized when surface charge q^1 is uniformly applied at the upper boundary of the piezoceramic while the stiffness at point P_2 is maximized. Figure 5 (b) shows the optimal configuration.

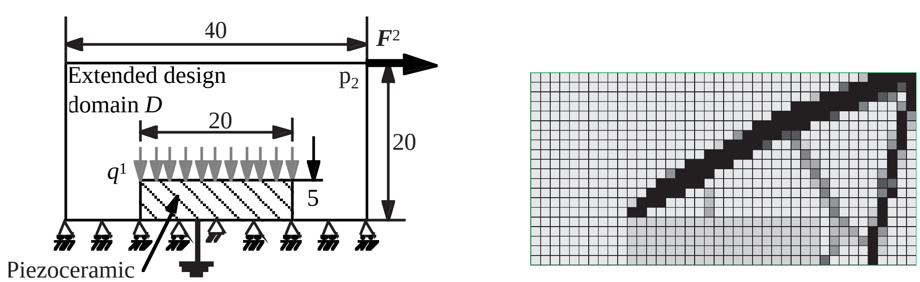

(a) Design domain

(b) Optimal configuration

Figure 5. Design of a flextensional actuator

Figure 6 (a) shows a design domain of a twisting actuator. The deformations at points P_{21}, P_{22}, P_{23}, and P_{24} in the directions of dummy loads $\boldsymbol{F}^{21}$, $\boldsymbol{F}^{22}$, $\boldsymbol{F}^{23}$, and $\boldsymbol{F}^{24}$, respectively are maximized when surface charge q^1 is uniformly applied at the upper boundary of the piezoceramic while the stiffnesses at point P_{21}, P_{22}, P_{23}, and P_{24} are maximized. Figure 6 (b) shows the optimal configuration. An image of a real structure is extracted from the optimal configuration as shown in Figure 6 (c). Figure 6 (d) shows the deformed shape of the actuator.

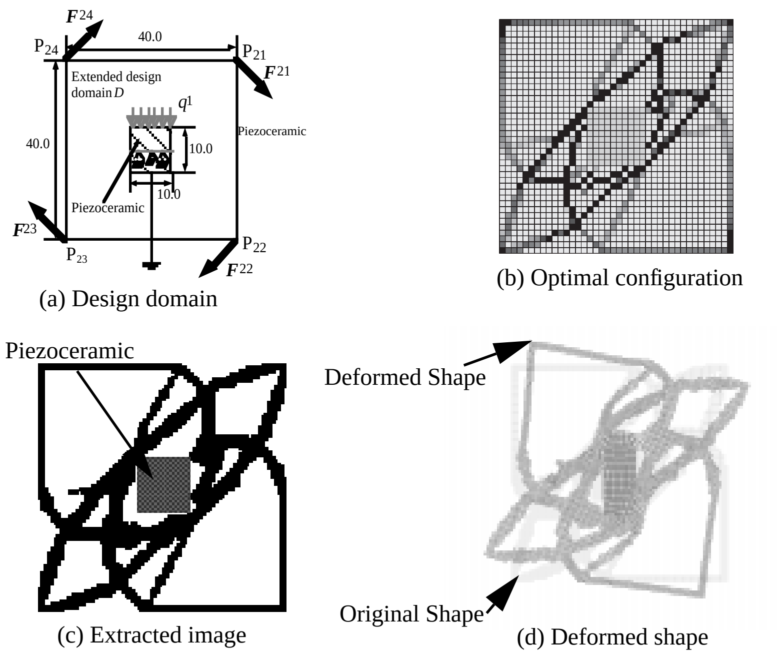

(a) Design domain (b) Optimal configuration

(c) Extracted image (d) Deformed shape

Figure 6. Design of a twisting flextensional actuator

<u>Design of Resonator</u>

Figure 7 (a) shows a design domain. We consider that the resonance condition which has to occur along a direction specified by a dummy load $\boldsymbol{F}^2$ at point P_2, when the periodically oscillating force along a direction specified by $\boldsymbol{F}^1$ is applied at point P_1. Table 1 shows the weighting coefficient, W in Equation (21), set in the optimization and the lowest eigen-frequencies of the optimal configurations**.** It is confirmed the lowest eigen-frequency of each optimal configurations matches the specified excitation frequency. Figure 7 (b), (c), and (d) show the optimal configurations in the case of ω=80, 200, and 400(Hz), respectively.

Table 1. Weighting coefficient W in Equation (21) and the lowest eigen-frequencies of the optimal configurations

$\omega/2\pi$ (Hz)	Initial configuration	W	Lowest eigen-frequency (Hz)
0	Uniform	0.5	29.39
80	0Hz	0.05	80.40
120	0Hz	0.05	119.28
160	120Hz	0.1	159.91
200	120Hz	0.2	200.32
240	120Hz	0.3	239.78
280	240Hz	0.4	280.80
320	240Hz	0.3	321.26
360	320Hz	0.3	359.62
400	320Hz	0.3	400.07

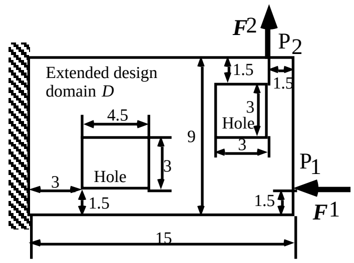

(a) Design domain

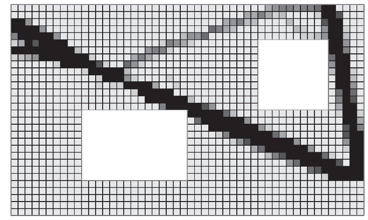

(b) Optimal configuration (ω=80(Hz))

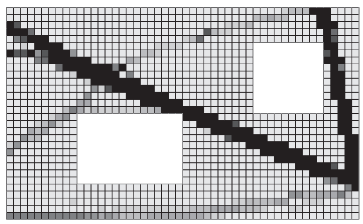

(c) Optimal configuration (ω=200(Hz))

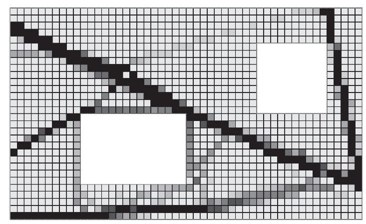

(d) Optimal configuration (ω=400(Hz))

Figure 7. Design of a resonator

8. Conclusions

The topology optimization method for the design of the flextensional actuators and resonators in MEMS was developed. The kinematic function was formulated using a mutual energy concept. A new multi-objective function was proposed in order to obtain an appropriate optimal configuration. Design examples confirmed that the method presented can be applied to the design of the flextensional actuators and resonators.

9. References

[1] Bendsøe, M. P. and Kikuchi, N. (1988). Generating optimal topologies in structural design using a homogenization method. *Computer Methods in Applied Mechanics and Engineering* 71, 197-224.

[2] Suzuki, K. and Kikuchi, N. (1991). A homogenization method for shape and topology optimization. *Computer Methods in Applied Mechanics and Engineering* 93, 291-318.

[3] Dogan, A. et al. (1997). Composite piezoelectric transducer with truncated conical endcaps “Cymbal”. *IEEE Transaction of Utrasonics, Ferroelectircs, and Frequency Contorl* 44-3, 597-605.

[4] Nguyen, C. T.-C. (1996). Micromechanical resonators for oscillators and filters. *Proc. of the 1995 IEEE Ultrasonics Symposium,* 489-499.

[5] Nishiwaki, S. (1998). Optimum structural topology design considering flexibility. *Ph.D. Dissertation. University of Michigan*.

[6] Pedersen, P. (1989). On optimal orientation of orthotropic materials. *Structural Optimization* 1, 101-106.